

Tetragonal and Orthorhombic Lattices of Martensites with Stable γ' precipitates — Calculations Based on Eshelby's Theory

by

Motozo HAYAKAWA* and Muneo OKA*

(Received May 31, 1980)

The lattice parameters and the elastic strain energies of martensites which include fine stable γ' precipitates have been calculated by using the Eshelby method. In the calculations, the γ' particles in a martensite plate were assumed not to transform to martensite. But a possibility of their deformation by a lattice invariant shear (LIS) due to the large internal stress was taken into account. The average lattice of a martensite varies from a tetragonal to orthorhombic lattice as the LIS increases. The elastic strain energy accumulated in a martensite plate is also reduced by a LIS. The results are successfully compared with the recent experimental data.

1 Introduction

The martensites of an Fe-Ni-Ti alloy have been reported to exhibit a tetragonal lattice, in spite of the absence of interstitial atoms¹⁻³). The tetragonality of this alloy has been attributed to the γ' precipitates, which form during an austenite aging or even during a quench. The γ' also stabilizes the austenite²⁻⁴). There are two different explanations proposed for these experimental observations.

In the first proposition^{3,4}) the γ' precipitates are assumed to transform to bcc martensite together with the surroundings. The reason why a bcc lattice, instead of a

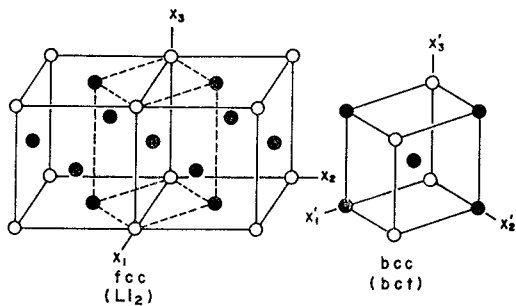


Fig. 1 Bain mechanism of an fcc to bcc lattice transformation (ignore the atom difference), and a formation of a bct lattice from $L1_2$ structure.

bcc, forms is shown in Fig. 1: The γ' has an ordered structure of the $L1_2$ type, in which the cube corners are occupied by Ti atoms and the face centers by Ni atoms. When this structure is transformed to martensite maintaining the Bain correspondence, the crystallographic symmetry of the resulting martensite becomes tetragonal. Along the c axis a lattice row consists of either

* Department of Mechanical Engineering

all Ti or all Ni, while along the a and b axes Ti and Ni atoms alternate. Since a Ti atom is larger than Ni, the c axis becomes longer than the a and b axes. As a result, the transformed γ' precipitate becomes bct. The rest of the region of a martensite plate is bcc by itself. However, because of the uniformly dispersed tetragonal centers of the transformed γ' , the entire martensite is elastically distorted. As an average the martensite lattice becomes tetragonal. The transformation of the γ' to bct is a result of mechanical forces by the surroundings. Therefore the existence of γ' precipitates requires an excess driving force for a martensite transformation. Thus, the transformation of γ' also explains the stabilization of the austenite.

In the second proposition^{4,5)}, the γ' precipitates are assumed not to transform; only the surrounding matrix transforms to martensite. Then a large stress field will be generated in a martensite plate because of a mismatching in shapes. The stress field would be such as to cause a tetragonal lattice of the martensite on an average. Since the transformation is possible only by surmounting this extra strain energy, a stabilization of the austenite would be expected.

Both the above propositions appear to explain the experimentally observed change in M_s temperature and the tetragonality of the martensite successfully, at least qualitatively. In order to decide which of these is really operative, a more quantitative analysis is needed. For the mechanism of the first proposition, since the dimensions of the hypothetical bct structure of γ' is not known, the average tetragonality of a martensite plate caused by the dispersed tetragonal centers cannot be estimated. Furthermore, since the chemical free energy of the hypothetical bct γ' is not known, the drop in M_s temperature cannot be estimated. On the other hand, the transformation mechanism in the second proposition can be dealt with by Eshelby's method⁶⁾, where an elastic state of a body with an ellipsoidal inclusion with a known transformation strain can be solved. In addition, a recent X-ray diffraction study⁷⁾ using a monocrystalline specimen has revealed an orthorhombic lattice of martensite in an Fe-Ni-Ti alloy. The orthorhombic lattice cannot be explained by the transformed γ' precipitates. However the second model may explain this when an additional lattice invariant shear (LIS) is introduced in the γ' precipitates. In the present paper, we attempt to calculate the average dimensions of the martensite plates with a uniform dispersion of non-transformed γ' precipitates. The results will be discussed in the light of some experimental observations.

2. procedure of calculations

The model we consider in this paper is as follows: The parent austenite contains uniformly dispersed spherical γ' precipitates. When this is cooled from the austenite state to a lower temperature, lenticular or plate-like martensites form. The γ'

particles contained in a martensite plate keep their original structure. As a result, a large stress and strain field will result in the plate. A possibility of a LIS in the γ' precipitates due to a large shear stress is also taken into account. In such a case we can calculate the average lattice of the martensite, the lattice orientation of the γ' and the elastic strain energy accumulated in the plate.

The same elastic state will result when the above mechanism is reversed; i.e., in an originally uniform martensite plate, spherical regions transform into the γ' structure and LIS may be introduced. This way of viewing the problem conforms to Eshelby's method⁶⁾. We will assume an elastically homogeneous and isotropic medium with Poisson's ratio of 1/3. Then, the only necessary parameter is the stress free strain (eigenstrain) of the spherical regions. Before we evaluate the strain components for the inverse transformation of the γ' , distortion matrices of various proposed mechanisms of martensitic transformation will be considered.

2.1 Matrix representation of martensitic transformations

According to the phenomenological theories^{8,9)}, a martensitic transformation consists of a lattice transformation, a LIS, and a rotation. Since the size of γ' precipitates is comparable to or smaller than the scale of inhomogeneity of a usual LIS*, this should not be included in the elastic interactions between the martensite and γ' particles. Without a LIS, several plausible mechanisms of the lattice transformation from fcc to bcc have been proposed (see e.g. refs. 10 and 11)

Bain mechanism

This is the simplest of all, yet very meaningful. Fig. 1 shows two fcc unit cells in juxtaposition (ignore the atom difference for the time being). The cell outlined by broken lines can be regarded as a bct unit cell, but its tetragonality is much higher than ordinary martensites. A compression along the vertical axis and a uniform expansion in the horizontal plane by a suitable amount will result in a martensite lattice (bcc or bct). The matrix representation referred to either fcc or bct axes is:

$$\mathbf{S}^B = \begin{pmatrix} \eta_1 & 0 & 0 \\ 0 & \eta_1 & 0 \\ 0 & 0 & \eta_3 \end{pmatrix} = \mathbf{B} \quad (1)$$

$$\text{with } \eta_1 = \sqrt{2}a/a_0, \eta_3 = c/a_0, \quad (2)$$

where, a_0 is the lattice constant of an fcc lattice, a and c are those of the bct. The lattice correspondence between the two lattices is:

$$({}_B \mathbf{C}_F) = \begin{pmatrix} 1 & -1 & 0 \\ 1 & 1 & 0 \\ 0 & 0 & 1 \end{pmatrix}, \quad (3)$$

* This LIS is different from the LIS in γ' considered in this paper.

and the following lattice orientation relationship results:

$$(0\ 0\ 1)_B \parallel (001)_F \text{ and } [100]_B \parallel [\bar{1}\bar{1}\ 0]_F .$$

Nishiyama mechanism

This mechanism is described in two steps. The shear in a $(1\ 1\ 1)_F$ plane toward a $[1\ 1\ \bar{2}]_F$ by $1/2\sqrt{2}$ results in a slightly distorted bcc lattice. A subsequent size adjustment keeping the $(1\ 1\ 1)_F$ plane fixed accomplishes the lattice transformation. The resulting orientation relationship is:

$$(0\ 1\ 1)_B \parallel (111)_F \text{ and } [\bar{0}\bar{1}\ 1]_B \parallel [1\ 1\ \bar{2}]_F .$$

The lattice correspondence is the same as Eq. (3).

Although the above procedure is a usual interpretation of the mechanism, as far as the initial and the final states are concerned, there is another way of describing the mechanism. Namely the Bain distortion followed by a rotation around the $[1\ \bar{1}\ 0]_F$ axis would result in exactly the same lattice and the same orientation. Therefore, the matrix representation of this mechanism referred to as the fcc lattice may be written:

$$\mathbf{S}^N = \mathbf{R}^N \mathbf{B}, \tag{4}$$

where,

$$\mathbf{R}^N = \begin{pmatrix} 1/\sqrt{2} & 1/\sqrt{6} & 1/\sqrt{3} \\ -1/\sqrt{2} & 1/\sqrt{6} & 1/\sqrt{3} \\ 0 & -2/\sqrt{6} & 1/\sqrt{3} \end{pmatrix} \begin{pmatrix} 1 & 0 & 0 \\ 0 & \cos \xi & \sin \xi \\ 0 & -\sin \xi & \cos \xi \end{pmatrix} \\ \times \begin{pmatrix} 1/\sqrt{2} & -1/\sqrt{2} & 0 \\ 1/\sqrt{6} & 1/\sqrt{6} & -2/\sqrt{6} \\ 1/\sqrt{3} & 1/\sqrt{3} & 1/\sqrt{3} \end{pmatrix}, \dots\dots\dots(5)$$

$$\text{and } \xi = \text{Tan}^{-1} a/c - \text{Tan}^{-1} 1/\sqrt{2} . \dots\dots\dots(6)$$

Kurdjumov and Sachs mechanism

This is similar to the Nishiyama mechanism. After the same first shear as the Nishiyama mechanism, a subsequent size adjustment takes place so that the following orientation relationship results:

$$(0\ 1\ 1)_B \parallel (111)_F \text{ and } [11\bar{1}]_B \parallel [1\ 0\ \bar{1}]_F .$$

Since this orientation of the martensite lattice can be obtained from the N orientation by a rotation around the $[1\ 1\ 1]_F$ axis, the K-S mechanism can be also expressed

by the Bain distortion followed by a rotation:

$$\mathbf{S}^{\text{K-S}} = \mathbf{R}^{\text{K-S}} \mathbf{B}, \quad (7)$$

where,

$$\mathbf{R}^{\text{K-S}} = \begin{pmatrix} 1/\sqrt{2} & 1/\sqrt{6} & 1/\sqrt{3} \\ -1/\sqrt{2} & 1/\sqrt{6} & 1/\sqrt{3} \\ 0 & -2/\sqrt{6} & 1/\sqrt{3} \end{pmatrix} \begin{pmatrix} \cos \xi - \sin \xi & 0 \\ \sin \xi & \cos \xi & 0 \\ 0 & 0 & 1 \end{pmatrix} \\ \times \begin{pmatrix} 1 & 0 & 0 \\ 0 & \cos \xi & \sin \xi \\ 0 & -\sin \xi & \cos \xi \end{pmatrix} \begin{pmatrix} 1/\sqrt{2} & -1/\sqrt{2} & 0 \\ 1/\sqrt{6} & 1/\sqrt{6} & 2/\sqrt{6} \\ 1/\sqrt{3} & 1/\sqrt{3} & 1/\sqrt{3} \end{pmatrix}, \quad \dots\dots (8)$$

and $\xi = \text{Sin}^{-1} 1/\sqrt{3} - 30^\circ = 5.26^\circ$.

Bogers and Burgers mechanism

This mechanism consists of two successive shears on non-parallel close packed planes. The orientation of the resulted bcc varies depending upon which planes are chosen for the shears. In fact, since the shear planes are not implied to be kept fixed, the orientation relationship is indeterminate. Yet the distortion matrix can be written by a product of the Bain distortion and a rotation:

$$\mathbf{S}^{\text{B-B}} = \mathbf{R}^{\text{B-B}} \mathbf{B}, \quad (9)$$

In all of the cases considered above, a distortion matrix can be expressed by the Bain distortion and a rotation. This is true for other mechanisms as long as the Bain correspondence holds. Since, as will be shown later, for a calculation of an elastic state, we need only the strain component (the symmetric part of a general distortion matrix); a rotation has no influence. Since \mathbf{B} is the symmetric part of distortion matrices and common to all cases, we don't have to distinguish between the above mechanisms. Regardless of which mechanism we assume for a martensitic transformation in a matrix, the resulting elastic state, including the orientation relationship, would be the same. Therefore we will use the Bain distortion as a representative transformation strain.

2.2 Inverse transformation of γ' from bcc to fcc lattice

Since the lattice transformation can be represented by the Bain distortion irrespective of the actual mechanism, the inverse lattice transformation can be expressed \mathbf{B}^{-1} . When a LIS is introduced in the inversely transformed fcc γ' lattice, the shape distortion of an original bcc γ' precipitates may be written:

$$\mathbf{S} = \mathbf{P}\mathbf{B}^{-1}, \tag{10}$$

where, \mathbf{P} is the LIS. In order to decide which shear system will be most likely to operate, a preliminary calculation has been made. $\{1\ 1\ 1\}_F$ planes are *a priori* chosen as probable shear planes. The highest shear stress on these planes has resulted in the system of $(1\ 1\ 1)\ (1\ 1\ \bar{2})_F$. Although there is no such shear system in an fcc metal, a combination of $1/2\ (1\ 0\ \bar{1})$ and $1/2\ (0\ 1\ \bar{1})$ is assumed. Therefore this system will be used for the LIS. Now the LIS can be expressed in the fcc basis:

$$({}_F\mathbf{P}_F) = \mathbf{I} + t \begin{pmatrix} 1/\sqrt{6} \\ 1/\sqrt{6} \\ -2/\sqrt{6} \end{pmatrix} (1/\sqrt{3}\ 1/\sqrt{3}\ 1/\sqrt{3}), \dots\dots\dots (11)$$

where, t is an amount of the LIS. It should be noted here that the maximum probable value of t is $1/2\sqrt{2}$, because at this value the shear stress subjected by the surroundings will be annulled.

Since it is convenient to make calculations on the bcc basis, Eq. (10) will be rewritten specifically on this basis using the Bowles and Mackenzie's notation.

$$({}_B\mathbf{S}_B) = ({}_B\mathbf{P}_B) ({}_B\mathbf{B}_B^{-1}) = ({}_B\mathbf{P}_B^{-1}) ({}_B\mathbf{C}_F) ({}_F\mathbf{P}_F) ({}_F\mathbf{C}_B) \tag{12}$$

A substitution of Eqs. (1), (3), and (11) into this equation results:

$$({}_B\mathbf{S}_B) = \begin{pmatrix} 1/\eta_1 & 0 & 0 \\ 0 & 1/\eta_1 & 0 \\ 0 & 0 & 1/\eta_3 \end{pmatrix} \begin{pmatrix} 1 & 0 & 0 \\ 0 & 1+2t/3\sqrt{2} & 2t/3\sqrt{2} \\ 0 & -2t/3\sqrt{2} & 1-2t/3\sqrt{2} \end{pmatrix}; \dots\dots (13)$$

$0 \leq t \leq 1/2\sqrt{2}$.

The above shape distortion matrix for a bcc γ' precipitate is non-symmetric. This can be factored into a symmetric part ($\bar{\mathbf{S}}$) and a rotation (β) (see for the procedure, e.g. ref. 12):

$$\mathbf{S} = \beta\bar{\mathbf{S}}. \tag{14}$$

For the elasticity problem, we need only the symmetric part $\bar{\mathbf{S}}$. In fact an eigenstrain is directly obtained from $\bar{\mathbf{S}}-\mathbf{I}$.

The β in Eq. (14) gives the lattice orientation of the γ' lattice relative to the surrounding martensite. This can be explained as follows: After an application of \mathbf{S} on a bcc γ' precipitate without the constraint of the surroundings, the lattice parallelism between the transformed γ' lattice and the surrounding martensite (Bain orientation relationship) will be maintained, since neither \mathbf{B} nor \mathbf{P} destroys the lattice parallelism. The removal of β for the calculation of an eigenstrain, however, causes a rotation of the γ' lattice by β^{-1} . An application of $\bar{\mathbf{S}}$ under the constraint of the

surroundings may also cause a rotation. However this does not happen when the transforming region is a sphere. Therefore β^{-1} gives the orientation of the γ' lattice with respect to the martensite lattice.

2.3 Eshelby's method

According to Eshelby⁵⁾, when an ellipsoidal region embedded in an infinitely large matrix undergoes a shape and size change, the stress and strain within the ellipsoid, and the total elastic strain can be calculated from the following set of equations:

$$e_{ij}^c = s_{ijkl} e_{kl}^T, \quad \dots\dots\dots (15)$$

$$d_{ij}^c = c_{ijkl} (e_{kl}^c - e_{kl}^T), \quad \dots\dots\dots (16)$$

$$E_{el} = -\frac{1}{2} d_{ij}^c e_{ij}^T V, \quad \dots\dots\dots (17)$$

where, the summation convention for repeated indices is implied. e_{ij}^c is the total (elastic plus plastic) strain of the ellipsoid under the constraint of the surroundings, e_{ij}^T is a stress free strain, or sometimes called an eigenstrain¹³⁾, of the ellipsoid. These are related by a fourth rank tensor called an Eshelby tensor, S_{ijkl} . when the region is a sphere, the Eshelby tensor becomes quite simple:

$$\begin{aligned} s_{1111} = s_{2222} = s_{3333} &= \frac{7-5\nu}{15(1-\nu)} = \frac{8}{15}, \\ s_{1122} = s_{2233} = s_{3311} &= -\frac{1-5\nu}{15(1-\nu)} = \frac{1}{15}, \quad \dots\dots\dots (18) \\ s_{1212} = s_{2323} = s_{3131} &= \frac{4-5\nu}{15(1-\nu)} = \frac{7}{30}, \end{aligned}$$

$$S_{ijkl} = 0, \text{ for other } ijkl,$$

where, the last terms are obtained by assuming Poisson's ratio is 1/3. Since $e_{kl}^c - e_{kl}^T$ is an elastic strain, a multiplication of this by the elastic stiffness constant, C_{ijkl} , yields the internal stress within the ellipsoid, σ_{ij}^l . E_{el} in Eq. (17) is the total (the ellipsoid plus the matrix) elastic strain energy, while V is the volume of the ellipsoid. Therefore, the elastic strain energy per unit volume of martensite, E , will be given by multiplying the volume fraction of the ellipsoidal region, f .

$$E = fE_{el}/V. \quad (19)$$

In the above equation, only an eigenstrain, except for the known constants, is needed for the calculation. The required eigenstrain is obtained from the following equation:

$$e_{ij}^T = \bar{S} - \mathbf{I}, \quad (20)$$

where, \bar{S} is the symmetric part of a shape distortion matrix defined by Eqs. (13) and

(14) , and \mathbf{I} is the unitary matrix.

2.4 Average lattice of the martensite

When a spherical region in a medium undergoes a shape change, the matrix is also strained. The strain field is not uniform and a calculation of the strain at an arbitrary point is generally difficult. However, if many particles with the same eigenstrain are uniformly distributed, the average strain of the entire body is simply given by:

$$\langle \gamma_{ij} \rangle_D = f e_{ij}^T, \tag{21}$$

where, $\langle \rangle_D$ denotes the average taken over the entire body (the particles plus the remaining matrix), and f is the volume fraction of the particles¹⁴. What we actually measure by X-ray diffraction, however, is the average over the matrix (martensite). The left hand side of Eq. (21) may be expressed by a weighted average of the average strain of the matrix ($\langle \gamma_{ij} \rangle_M$) and that of the particles ($\langle \gamma_{ij} \rangle_D$), i.e.,

$$\langle \gamma_{ij} \rangle_D = (1-f) \langle \gamma_{ij} \rangle_M + f \langle \gamma_{ij} \rangle_D,$$

or rewriting the last term,

$$\langle \gamma_{ij} \rangle_D = (1-f) \langle \gamma_{ij} \rangle_M + f S_{ijkl} e_{kl}^T. \tag{22}$$

By equating the right hand sides of Eqs. (21) and (22) , the average strain of the martensite can be obtained:

$$\langle \gamma_{ij} \rangle_M = \frac{f}{1-f} (e_{ij}^T - S_{ijkl} e_{kl}^T). \tag{23}$$

From this, the dimensions of the average martensite can be calculated. In the present case only $\langle \gamma_{11} \rangle$, $\langle \gamma_{22} \rangle$, $\langle \gamma_{33} \rangle$, and $\langle \gamma_{23} \rangle$ are non-zero. Therefore, the dimensions of the average martensite becomes a monoclinic lattice. That is :

$$\begin{aligned} a &= 1 + \langle \gamma_{11} \rangle_M, \\ b &= \sqrt{(1 + \langle \gamma_{22} \rangle_M)^2 + \langle \gamma_{23} \rangle_M^2}, \\ c &= \sqrt{(1 + \langle \gamma_{33} \rangle_M)^2 + \langle \gamma_{23} \rangle_M^2}, \\ \alpha &= 90 - 2 \text{Tan}^{-1} \langle \gamma_{23} \rangle_M, \end{aligned} \tag{24}$$

where, α is the angle between the b and c axes. Since α is nearly equal to 90°, an orthorhombic lattice is a fair approximation.

3. Results and discussion

Calculations have been made for an Fe-30Ni-3.5Ti alloy. A complete precipitation was assumed, resulting in $f = 0.165$. For the calculation of the Bain distortion in Eq. (1), the lattice parameters of Fe-31Ni were used, i.e., $a_0 = 0.3591\text{nm}$ and $a = 0.2875\text{nm}$ ¹⁵⁾. This is because the measured parameters of Fe-Ni-Ti alloy are already influenced by the γ' precipitations, and not adequate for the calculation of eigenstrains.

Components of the calculated eigenstrains referred to the martensite basis for various amount of LIS are listed in Table 1. Components not listed are all zero.

Table 1 The eigenstrains and the rotation angles of the γ' lattice

x ^{*1}	$\begin{matrix} T \\ e_{11} \end{matrix}$	$\begin{matrix} T \\ e_{22} \end{matrix}$	$\begin{matrix} T \\ e_{33} \end{matrix}$	$\begin{matrix} T \\ e_{23} \end{matrix}$ ^{*2}	β ^{*3}
0.0	-0.1168	-0.1168	0.2490	0.0	0.0
0.1		-0.1019	0.2283	-0.0058	0.96
0.2		-0.0865	0.2077	-0.0110	1.92
0.3		-0.0707	0.1873	-0.0157	2.89
0.4		-0.0544	0.1671	-0.0197	3.86
0.5		-0.0378	0.1471	-0.0231	4.83
0.6		-0.0208	0.1273	-0.0259	5.81
0.7		-0.0034	0.1078	-0.0281	6.79
0.8		0.0143	0.0885	-0.0297	7.77
0.9		0.0324	0.0695	-0.0306	8.75
1.0		0.0508	0.0508	-0.0309	9.74

*1 $x = t/2\sqrt{2}$, where t is an amount of LIS in an fcc lattice

*2 Components are referred to the martensite lattice basis. Those not listed are all zero.

*3 Rotation is around the $[100]_B$ axis (in deg).

Since the rotations of the γ' lattice relative to the martensite were around the $[1\ 0\ 0]_B$ axis (see Eq. (14)), only the angles of these rotation are sufficient to describe β . The angles of the rotation are listed in the last column. Using these eigenstrains, the lattice parameters of the average martensite have been calculated from Eqs. (23) and (24) for each amount of LIS. The calculated parameters are relative to the parameters of unstressed martensite. Elastic strain energies have been also calculated from Eqs. (15)–(17) and (19). The results are summarized in Table 2. These are also plotted in Fig. 2. A development of an orthorhombic lattice and a reduction in the strain energy with an increasing LIS are clearly seen.

Now, in order to examine the plausibility of the present model, the results will be compared with some recent experimental data. Lysak et al.⁷⁾ used a monocrystalline specimen of an Fe-31Ni-5.3Ti for X-ray diffraction and measured a change of the

lattice parameters of martensites with the time of aging at 700°C. Fig. 3 is a reproduction of their result. A tetragonality is already seen even in as quenched mart-

Table 2 Relative parameters of the average martensite and elastic strain energies of martensite

x	a	b	c	α *1	E *2
0.0	0.9875	0.9875	1.0260	90.00	$7.87 \times 10^{-3} \mu$
0.1	0.9876	0.9891	1.0239	90.07	6.72
0.2	0.9876	0.9908	1.0218	90.13	5.68
0.3	0.9877	0.9926	1.0197	90.19	4.83
0.4	0.9877	0.9943	1.0177	90.24	3.99
0.5	0.9878	0.9961	1.0156	90.28	3.33
0.6	0.9878	0.9979	1.0136	90.31	2.79
0.7	0.9879	0.9998	1.0115	90.34	2.38
0.8	0.9879	1.0017	1.0095	90.36	2.08
0.9	0.9879	1.0036	1.0075	90.37	1.90
1.0	0.9879	1.0056	1.0056	90.37	1.83

*1 Angle between the b and c axes (in deg)

*2 Elastic strain energy in a unit of shear modulus μ

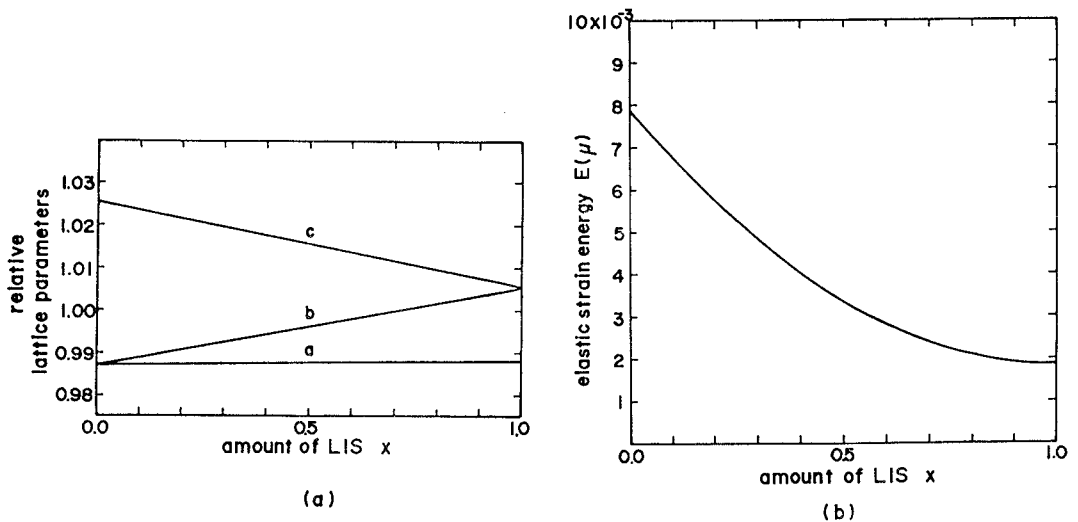


Fig. 2 Variation of the relative lattice parameters (relative to the unstressed martensite) (a), and the elastic strain energy per unit volume of martensite (b), with the amount of LIS x ($x = t/2\sqrt{2}$).

ensites. The tetragonality increases rapidly and reaches a maximum in 30 min. The quick increase of the tetragonality to this point is attributed to the rapid development of the γ' precipitation. In this alloy it has been reported⁽⁶⁾ that an Ostwald ripening of the γ' starts in an hour, at latest; possibly starts earlier if the measurement could

be done in the early stage. Therefore, after 30 min of aging the precipitation reaction can be assumed to be completed, i.e., the assumption made in the present calculation is fulfilled. Therefore the present results should be compared with the data in Fig. 3 at and longer than 30 min of aging. The maximum tetragonality in Fig. 3 is 1.036, in accordance with the maximum tetragonality of the present result (1.039). The development of the orthorhombic lattices may be also explained, if the aging time is correlated to the amount of LIS.

In the present calculation, the LIS was assumed to be homogeneous, although a shear by slips is inhomogeneous on an atomistic scale. The degree of the inhomogeneity is dominant especially when the size of γ' precipitates is small. When a particle size is less than, say 1.2nm, only a single slip by the Burgers vector ($a/2 [1 \ 1 \ \bar{2}]$) will exceed the maximum allowable LIS. In such a case, a LIS is prohibited in the particle. As a particle grows, the number of probable slip planes increases. If this is interpreted as a measure of ease of shearing, the amount of LIS is correlated to the size of γ' precipitates. Furthermore, since the γ' growth follows the Ostwald ripening, the average radius increases proportionally to $[\text{aging time}]^{1/3}$ ¹⁷⁾. This explains the development of the orthorhombic lattice and why the change occurs quickly at the beginning and slows down later. Comparing the lattice parameters in Fig. 2 and Fig. 3, the LIS appears never to reach its maximum. The increasing slowness of the growth of the γ' may not be sufficient for an explanation. According to Fig. 2, the elastic strain energy is more effectively reduced for smaller LIS. In addition, when γ' precipitates grow large, other mechanism of strain accommodation may come into play. These might be additional reasons for the immature LIS.

Fig. 4 shows the variations of the M_s temperature with the aging time after Abraham and Pascover³⁾. Although the alloy composition is different

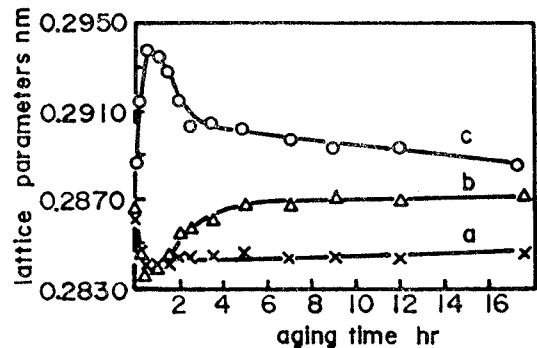


Fig. 3 Dependence of the lattice parameters of martensite on the time of austenite aging at 700°C (Fe-31Ni-5Ti), after ref. (7).

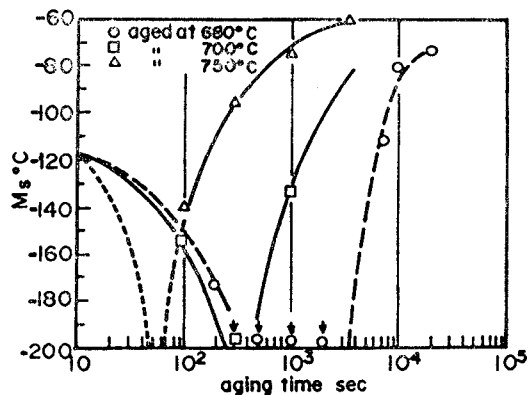


Fig. 4 Dependence of M_s on the time of austenite aging (Fe-29.5Ni-4Ti), after ref. (3).

from the previous one, the time for the minimum M_s temperature (aged at 700°C) is well correlated to that for the maximum tetragonality in Fig. 3. Thus, the quick drop of the M_s temperature to its minimum is similarly attributed to the fast development of the γ' precipitates. Beyond this point, as the γ' precipitates grow the amount of LIS increases causing a reduction in the elastic strain energy (Fig. 2). This will explain the elevation of the M_s temperature in Fig. 4.

Lattice rotations of the γ' have also been observed¹⁸⁾ in electron diffraction patterns. Their explanation of the rotation is somewhat different from ours. Since only the projected angles have been recorded, a detailed comparison with the present results cannot be made.

In the present model, a LIS was assumed to occur only in γ' precipitates to reduce the high stress field caused by the large misfits. However, a LIS may occur in the surrounding martensite or in both of the phases. In such cases the calculation would become considerably laborious. However, as long as the LIS is localized in the neighbourhood of the γ' precipitates, the results would not be very different from the present results.

4. Conclusions

The average lattice and the elastic strain energy of Fe-Ni-Ti martensite have been calculated. Where, it was assumed that : a) the γ' precipitates do not transform during the martensitic transformation of the surrounding matrix, b) but these may plastically deform by slips due to the large internal stress. We have been led to the following conclusions :

1) When the γ' precipitates do not deform (neither by lattice transformation nor by slips), the martensite containing these particles becomes tetragonal and the elastic strain energy accumulated in the martensite is high.

2) When the γ' precipitates deform by slips, the martensites becomes orthorhombic and the strain energy is reduced.

3) The transition from (1) to (2) may be correlated to the size of γ' precipitates, since when the precipitates are small, say less than 1.2nm, a slip is prohibited, but as they grow these can be sheared.

4) The results are generally in good agreement with experimental observations, supporting the plausibility of the present model.

References

- 1) Y. Honnorat, G. Henry and J. Manenc, *Mémoires Scientifiques Rev. Metallurg.*, **62**, 429 (1965)
- 2) Y. Honnorat, G. Henry, G. Murry and J. Manenc, *C. R. Acad. Sc. Paris*, **260**, 2214 (1965)
- 3) J. K. Abraham and J. S. Pascover, *Trans. AIME*, **245**, 759 (1969)
- 4) E. Hornbogen and W. Meyer, *Acta Met.*, **15**, 584 (1967)
- 5) M. M. Hall and P. G. Winchell, *Acta Met.*, **25**, 735 (1977)
- 6) J. D. Eshelby, *Proc. Roy. Soc.*, **A241**, 376 (1957)
- 7) L. I. Lysak, S. P. Kondrat'yev and V. S. Tatarchuk, *Phys. Met. Metallogr.*, **42**, No. 2, 101 (1976)
- 8) J. S. Bowles and J. K. Mackenzie, *Acta Met.*, **2**, 129 (1954), *ibid.*, **2**, 138 (1954)
- 9) M. S. Wechsler, D. S. Lieberman and T. A. Read, *Trans. AIME*, **197**, 1503 (1953)
- 10) Z. Nishiyama, *Martensitic Transformations*, Maruzen, Tokyo (1971)
- 11) A. J. Bogers and W. G. Burgers, *Acta Met.*, **12**, 255 (1964)
- 12) C. M. Wayman, *Introduction to the Crystallography of Martensitic Transformations*, MacMillan Co., New York (1964)
- 13) T. Mura, *Advances in Materials Research* (edited by H. Herman), Vol. 3, Wiley, New York (1968)
- 14) T. Mura and T. Mori, *Micromechanics*, Baifukan, Tokyo (1976)
- 15) J. F. Breedis and C. M. Wayman, *Trans. AIME*, **224**, 1128 (1962)
- 16) I. L. Cheng and G. Thomas, *Met. Trans.*, **3**, 503 (1972)
- 17) K. Hirano, *Precipitations in Alloys* (edited by Y. Koda), Chapt. 6, Maruzen, Tokyo (1972)
- 18) T. Maki and C. M. Wayman, *Acta Met.*, **25**, 695 (1977)